# THE MINIMAL ENTROPY PRIOR FOR SIMULTANEOUS RECONSTRUCTION AND SEGMENTATION OF IN VIVO MICROCT TRABECULAR BONE IMAGES

*M. Depypere*[*], *J. Nuyts*[†], *K. Laperre*[‡], *G. Carmeliet*[‡], *F. Maes*[*], *P. Suetens*[*]

[*]Medical Image Computing (ESAT/PSI), [†]Department of Nuclear Medicine,
[‡]Laboratory for Experimental Medicine and Endocrinology,
Katholieke Universiteit Leuven, Leuven, Belgium

## ABSTRACT

We present the minimal entropy prior for the iterative reconstruction of $\mu$CT projection data using the maximum a posteriori (MAP) framework. The minimal entropy prior restricts the number of intensity values in the reconstruction without requiring a priori information about the number of image tissues or tissue intensity estimates. We utilise the presented prior in the MAP framework to simultaneously reconstruct and segment trabecular bone from low quality $\mu$CT images. The MAP approach allows the straightforward incorporation of the in vivo scanner point spread function, while the entropy prior yields a segmentation that obeys to projection data.

***Index Terms***— Image reconstruction, image segmentation, transmission tomography, $\mu$CT, entropy

## 1. INTRODUCTION

Quantitative information on small animal trabecular bone structures is of major interest for bone research. The information is typically gathered by acquiring micro computed tomography ($\mu$CT) images of small animal models. The quantitative measures are calculated from binary images, requiring segmentations of the obtained images. The segmentation can be adversely affected by resolution effects, as is the case for in vivo imaging. Thin trabecular bone structures of mice have dimensions similar to the system resolution, leading to blurred and less intense trabeculae in the reconstructions [1].

In vivo imaging allows performing longitudinal studies, to evaluate differences in bone architecture over time. Hence, it is of importance that the segmentation is sufficiently accurate to detect subtle alterations. Global and local adaptive thresholding methods have been proposed, but these generally ignore the effect of the modulation transfer function (MTF), or take it into account heuristically [2]. To obtain more accurate segmentations one can include the projection data in the segmentation, allowing the modelling of the point spread function (PSF) of the scanner system. This has led to the recent development of measures such as the minimum projection distance, where the quality of a segmentation is determined by the difference between projections of the segmentation and the measured projection data [3].

As the segmentation is linked to the quality of the reconstruction, we instead pursue the simultaneous reconstruction and segmentation (SRS) approach. In these methods the maximum a posteriori (MAP) framework is used to generate a reconstruction that agrees with the data in a statistical sense, and that is regularised to reduce the noise in the reconstruction. The MAP approach allows the straightforward incorporation of the in vivo scanner PSF and hence to correct the effect of the MTF. Additionally the MAP approach allows the regularisation to restrict the number of intensity values, resulting in a segmented reconstruction. Other SRS methods have relied on mixed Gaussian or gamma distribution priors to model the different tissues in the image [4, 5]. A disadvantage of such priors is that the number of tissues in the image needs to be known before reconstructing, and estimates of the mean and standard deviation of the intensities of the tissue classes need to be supplied. Mutual information and joint entropy have been applied to account for anatomical information in PET reconstruction [6, 7]. We adapt the joint entropy prior proposed in [8] and use it to overcome the limitations presented by the tissue modelling priors.

First, the MAP framework will be revisited, after which the minimal entropy prior will be introduced. The presented method is then validated on in vivo $\mu$CT images of real mouse tibiae, with the corresponding high resolution ex vivo $\mu$CT images as ground truth. We illustrate the advantage of the PSF modelling and compare the segmentation produced by the minimal entropy prior to those of the mixed distribution prior and the conventional local thresholding.

## 2. METHODS

### 2.1. The MAP equation

The general form of a MAP reconstruction is given by

$$\mu = \arg\max_{\mu} \ln P(y|\mu) + \ln P(\mu) \qquad (1)$$

with $\mu$ the transmission data to be reconstructed and $y$ the measured sinogram. Using a Poisson data model, the loga-

rithm of the likelihood, denoted as $L$, of transmission scans is given by [9]

$$L = \ln P(y|\mu) \quad (2)$$
$$= \sum_i y_i \ln\left(b_i e^{-p_i} + s_i\right) - \left(b_i e^{-p_i} + s_i\right) \quad (3)$$

with $p_i = \sum_j l_{ij}\mu_j$. The number of photon counts of sinogram ray $i$ is given by $y_i$, $b_i$ represents the number of photon counts in the blank sinogram ray $i$, $s_i$ the scatter in ray $i$, $l_{ij}$ the intersection length of sinogram ray $i$ with voxel $j$, and $\mu_j$ the reconstructed attenuation value in pixel $j$. The projections $p_i$ are computed using a projector. The system PSF can be incorporated into the projector by smoothing the calculated sinogram with the PSF after projecting and before backprojecting. It is known that image detail converges faster if the smoothing is omitted in the backprojector [10]. This also increases noise propagation, but this is limited to the first iterations, after which we do perform the smoothing, and counteracted with the prior.

### 2.2. Selection of the prior

The prior information about the reconstructed image is usually of the form

$$N = \ln P(\mu) = -\beta M(\mu) \quad (4)$$

with $\beta$ a parameter to control the weight of the prior. Setting $\beta = 0$ reduces the MAP equation to the maximum likelihood (ML) equation, which has a noisy solution. We are interested in a prior that will also restrict the number of intensity values in the reconstruction to obtain a segmentation.

#### *2.2.1. Mixed distribution prior*

An often used prior for segmentation is the mixed distribution prior. If the number of tissues in the image and the mean and variance of their intensities are known, the image histogram can be modelled with a number of Gaussian or gamma distributions. In the case of Gaussian mixtures, the mixed distribution prior is

$$M_{\mathrm{MD}}(\mu) = \sum_j \frac{(\mu_j - \mu_{l_j})^2}{2\sigma_{l_j}^2} - \ln\sqrt{2\pi}\sigma_{l_j} \quad (5)$$

with $l_j \in \{1, 2, ..., t\}$ the label of pixel $j$, which can be one of $t$ tissues, and $\mu_t$ and $\sigma_t$ the mean and standard deviation of the intensities of image tissue $t$. The parameters $\mu_t$ and $\sigma_t$ can be successively refined after an estimate is supplied to initialise the prior.

We apply the implementation of the mixed distribution prior as presented in Appendix B of [11]. We successively update the mean intensities but keep the standard deviations fixed.

#### *2.2.2. Minimal entropy prior*

Instead of modelling the different tissues, we propose to use the minimal entropy prior as segmentation prior. A joint entropy prior is proposed in [8], where the prior minimises the joint entropy of the current reconstruction and an anatomical prior image. Minimizing the joint entropy will encourage clusters to form in the joint histogram. It was illustrated that this clustering also occurs when no anatomical information is known, and a uniform anatomical image is used. In this case the joint entropy reduces to the entropy of the current reconstruction. Thus we are effectively using a minimal entropy prior.

The minimal entropy prior is defined as

$$M_{\mathrm{ME}}(\mu) = -\sum_a p_\mu(a) \ln p_\mu(a) \quad (6)$$

with $p_\mu(a)$ the normalised histogram, i.e. the probability of image intensity bin $a$ in $\mu$. To ensure differentiability, $p_\mu$ is calculated using a Parzen window estimator

$$p_\mu(a) = \frac{\sum_j p_{\mu_j}(a)}{\sum_a \sum_j p_{\mu_j}(a)}, \text{with} \quad (7)$$
$$p_{\mu_j}(a) = \frac{1}{\sqrt{2\pi}\sigma} e^{\frac{-(\mu_j - a)^2}{2\sigma^2}} \quad (8)$$

$\sigma$ is the standard deviation of the Gaussian of the Parzen window. Increasing the value of $\sigma$ leads to a lower number of independent bins, and has a similar effect as decreasing $a$. We consider $\sigma$ and $a$ as parameters to be fixed a priori.

The gradient of the minimal entropy prior is given by

$$\frac{\partial M_{ME}}{\partial \mu_j} = -\sum_a (1 + \ln p_\mu(a)) p_{\mu_j}(a) \frac{a - \mu_j}{\sigma^2} \quad (9)$$

As in [8] we approximate the second derivative heuristically to

$$\frac{\partial^2 M_{ME}}{\partial \mu_j^2} \approx \sum_a \frac{\ln p_\mu(a) p_{\mu_j}(a)}{\sigma^2}. \quad (10)$$

The minimal entropy prior is not concave and introduces local maxima. To avoid undesired local minima, we increase the strength of the prior gradually during iterations [8].

### 2.3. Solving the MAP equation

To solve equation (1) for $\mu$ we use the implementation of [12]. Defining the logarithm of the prior as $N$, this leads to the updating formula:

$$\mu_j = \mu_j^{\mathrm{old}} + \left(\frac{\partial L}{\partial \mu_j} + \frac{\partial N}{\partial \mu_j}\right) / \left(\frac{\sum_i l_{ij}}{\mu_j^{\mathrm{old}}} - \frac{\partial^2 N}{\partial \mu_j^2}\right) \quad (11)$$

$\mu_j$ and $\mu_j^{old}$ are the new and current reconstructed attenuation values in pixel $j$. All partial derivatives are evaluated in the current reconstruction.

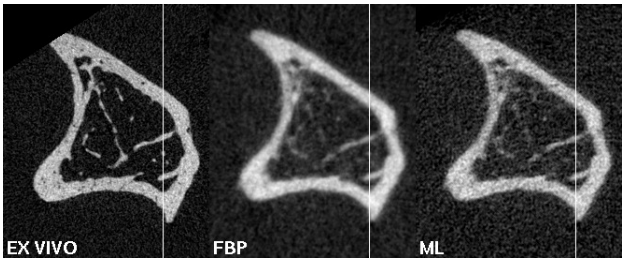


(a) Reconstructions obtained with each method.

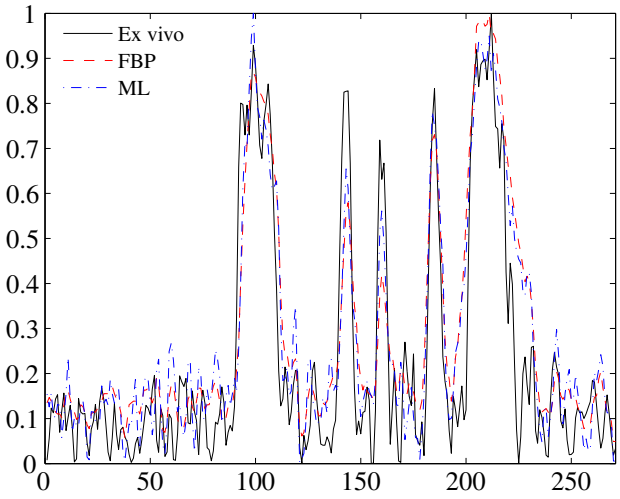


(b) Profiles corresponding to the vertical lines in (a).

**Fig. 1**. Illustration of the influence of the PSF modelling on the reconstruction. Shown are the ground truth (Ex vivo), and reconstructions by the filtered backprojection method (FBP), and by the iterative approach with PSF modelling (ML).

## 3. EXPERIMENTS

The method was evaluated in the context of the segmentation of trabecular bone of in vivo $\mu$CT images of mice. Five mouse tibiae were scanned in vivo (SkyScan1076, 50kV, 100$\mu$A, 3300ms, 1mm Al, 8.73$\mu$m pixelsize, 1° stepsize, 180° rotation). The mice were immediately sacrificed and the excised tibiae were scanned one day later ex vivo at higher resolution (SkyScan1172, 50kV, 200$\mu$A, 590ms, 0.5mm Al, 4.89$\mu$m pixelsize, 0.71° stepsize, 180° rotation).

To determine the effect of the PSF correction the in vivo projection data were reconstructed with the filtered backprojection software provided with the $\mu$CT scanner (NRecon, SkyScan). In addition, the in vivo projections were reconstructed with the ML approach ($\beta = 0$). The ex vivo projections were reconstruced using the NRecon software and registered to the in vivo reconstructions to serve as ground truth of the bone. The resulting reconstructions of one animal are shown in figure 1a. The ML reconstruction is noisier but this is of no concern as in practice it will be regularised with a prior. The profiles corresponding to the vertical lines plotted in figure 1b illustrate that the PSF modelling in the MAP framework improves the intensities of thin trabecula with respect to the filtered backprojection.

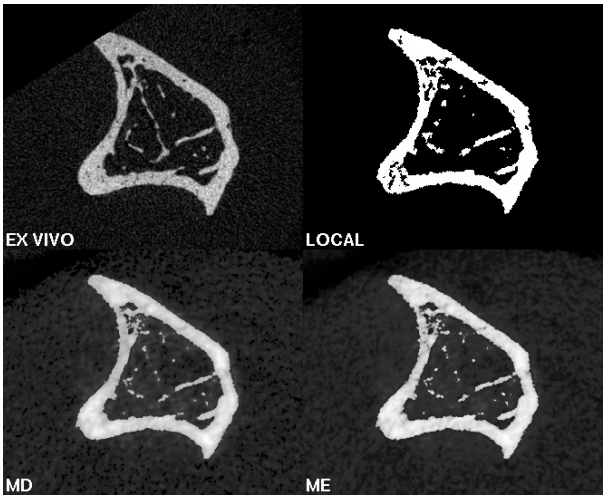


**Fig. 2**. Comparison of segmentation results. The top row shows the ex vivo ground truth and the local thresholding method. The bottom row shows the results of the presented method with the mixed distribution (MD) and minimal entropy (ME) priors.

To evaluate the quality of the resulting segmentation, we compare the presented method with the ex vivo ground truth and the local thresholding method described by Waarsing et al. [2], which is frequently used for bone segmentation. These images of the same animal as before can be seen in the top row of figure 2. The in vivo projection data were simultaneously reconstructed and segmented with the presented method and priors. Parameter estimates $\mu_t$ and $\sigma_t$ of the mixed distribution prior were derived from the ML reconstruction, while minimal entropy prior parameter $\sigma$ was fixed to $\sigma = 1$ bin and $a$ chosen from 50 or 70 bins. The bottom row of figure 2 shows these segmentations with left the mixed distribution prior and right the minimal entropy prior. It can be seen that both priors induce a similar segmentation, and that they outperform the local thresholding method with respect to detecting and rendering thin trabeculae.

For a quantitative evaluation, we calculated the bone volume ratio, trabecular thickness and trabecular number from the segmented images. The same 2D region of interest was used for both the ex vivo image as for the in vivo reconstructions. Because both segmentation methods sometimes overestimated and sometimes underestimated bone characteristics, the root mean square value was used to average percentage errors over different bone samples. As can be seen in table 1, the root mean square errors from the ground truth improved for the three bone characteristics with the presented minimal entropy prior segmentation.

The computation time of the first and second derivatives

| Segmentation | BV/TV | Tr.Th | Tr.N |
|---|---|---|---|
| Local | 22.43 | 9.70 | 17.05 |
| Minimal Entropy | 6.42 | 6.61 | 7.82 |

**Table 1**. Root mean square values of the percentage errors from the ground truth for bone volume ratio (BV/TV), trabecular thickness (Tr.Th) and trabecular number (Tr.N), for two segmentation methods.

of the minimal entropy prior takes 10 times longer than those of the mixed distribution prior with the current serial implementation. Every pixel needs to be distributed over the histogram by the Parzen window, requiring multiple times the computation power per pixel compared to the mixed distribution prior. This results in a total reconstruction time that is twice as long for the miminal entropy prior compared to the mixed distribution prior.

## 4. CONCLUSION

We have presented the minimal entropy prior that restricts the number of intensity values in a reconstruction without requiring tissue information. We have applied the presented prior in the MAP framework to the segmentation of low quality in vivo $\mu$CT images of murine trabecular bone. This provides several advantages over traditional techniques. If the PSF of the scanner is known it can be taken into account, significantly improving the reconstruction. In addition the choice of the prior allows to simultaneously reconstruct and segment the projection data. We have shown that the resulting segmentation corresponds with the actual high quality measurement of the bone and that the results of the minimal entropy prior are similar to mixed distribution priors, but using more generic assumptions.

In addition to the segmentation of low quality trabecular bone, the minimal entropy prior can be applied to bone images that contain variations in degree of bone mineralisation and have a priori unknown attenuation values. Besides these exemplary cases in the bone field, the minimal entropy prior could prove useful in many other applications.

## 5. REFERENCES


[1] S. T. Witt, C. H. Riedel, M. Goessl, M. S. Chmelik, and E. L. Ritman, "Point spread function deconvolution in 3D micro-CT angiography for multiscale vascular tree separation," in *Society of Photo-Optical Instrumentation Engineers (SPIE) Conference Series*, June 2003, vol. 5030, pp. 720–727.

[2] J.H. Waarsing, J.S. Day, and H. Weinans, "An improved segmentation method for in vivo microct imaging," *Journal of Bone and Mineral Research*, vol. 19, no. 10, pp. 1640–1650, 2004.

[3] K.J. Batenburg and J. Sijbers, "Optimal threshold selection for tomogram segmentation by reprojection of the reconstructed image," in *CAIP*, 2007, vol. 4673 of *Lecture Notes in Computer Science*, pp. 563–570.

[4] Ing-Tsung Hsiao, A. Rangarajan, and G. Gindi, "Joint-map bayesian tomographic reconstruction with a gamma-mixture prior," *Image Processing, IEEE Transactions on*, vol. 11, no. 12, pp. 1466–1477, Dec 2002.

[5] D. Van de Sompel and M. Brady, "Simultaneous reconstruction and segmentation algorithm for positron emission tomography and transmission tomography," *ISBI 2008*, pp. 1035–1038, May 2008.

[6] S. Somayajula, E. Asma, and R.M. Leahy, "Pet image reconstruction using anatomical information through mutual information based priors," *Nuclear Science Symposium Conference Record, 2005 IEEE*, vol. 5, pp. 2722–2726, Oct. 2005.

[7] Jing Tang, B.M.W. Tsui, and A. Rahmim, "Bayesian pet image reconstruction incorporating anato-functional joint entropy," *ISBI 2008*, pp. 1043–1046, May 2008.

[8] J. Nuyts, "The use of mutual information and joint entropy for anatomical priors in emission tomography," *Nuclear Science Symposium Conference Record, 2007. NSS '07. IEEE*, vol. 6, pp. 4149–4154, 26 2007-Nov. 3 2007.

[9] K. Lange and R. Carson, "EM reconstruction algorithms for emission and transmission tomography," *Journal of Computer Assisted Tomography*, vol. 8, no. 2, pp. 306–316, April 1984.

[10] G.L. Zeng and G.T. Gullberg, "Unmatched projector/backprojector pairs in an iterative reconstruction algorithm," *Medical Imaging, IEEE Transactions on*, vol. 19, no. 5, pp. 548–555, May 2000.

[11] J. Nuyts, P. Dupont, S. Stroobants, R. Benninck, L. Mortelmans, and P. Suetens, "Simultaneous maximum a posteriori reconstruction of attenuation and activity distributions from emission sinograms," *Medical Imaging, IEEE Transactions on*, vol. 18, no. 5, pp. 393–403, May 1999.

[12] J. Nuyts, D. Beque, P. Dupont, and L. Mortelmans, "A concave prior penalizing relative differences for maximum-a-posteriori reconstruction in emission tomography," *Nuclear Science, IEEE Transactions on*, vol. 49, no. 1, pp. 56–60, Feb 2002.